Theor Chem Acc (2004) 112: 453–459
DOI 10.1007/s00214-004-0615-y

Theoretical
Chemistry Accounts

Regular article

Electron localizability indicator for correlated wavefunctions. I. Parallel-spin pairs

Miroslav Kohout[1], **Katarzyna Pernal**[1,2], **Frank Richard Wagner**[1], **Yuri Grin**[1]

[1] Max-Planck-Institut für Chemische Physik fester Stoffe, Nöthnitzer Str. 40, 01187 Dresden, Germany
[2] Institute of Physics, University of Szczecin, Wielkopolska 15, 70-451 Szczecin, Poland

Received: 1 April 2004 / Accepted: 8 September 2004 / Published online: 13 November 2004

Abstract. The electron localizability indicator (ELI) is based on a functional of the same-spin pair density. It reflects the correlation of the motion of same-spin electrons. In the Hartree–Fock approximation the ELI can be related to the electron localization function (ELF). For correlated wavefunctions the ELI formula differs from the one for the ELF.

Keywords: Electron localizability indicator–Configuration interaction–Electron localization function

1. Introduction

Various descriptors are used to analyze the bonding situation for molecules and solids in real space. Those descriptors are functions or functionals of the many-electron wavefunction obtained from a quantum mechanical calculation. Over the past decade the electron localization function (ELF) has earned growing popularity, especially among chemists. The original ELF formula of Becke and Edgecombe ($\mathrm{ELF_{BE}}$), derived at the Hartree–Fock (HF) level of theory, is based on the curvature of the spherically averaged same-spin conditional pair probability density [1]. Because the electron pair density is not accessible from a density functional calculation, the wide acceptance and application of the ELF would not have been possible without the alternative definition of ELF by Savin et al. ($\mathrm{ELF_S}$) [2] based on the Pauli kinetic energy density of noninteracting electrons, i.e., using Kohn–Sham orbitals.

Neither the curvature of the spherically averaged same-spin conditional pair probability density nor the Pauli kinetic energy density provide the specific features utilizable in the bonding analysis. It is the (arbitrarily chosen) reference to the uniform electron gas that gives rise to the richness of chemical information so typical for ELF. Unfortunately, this uniform electron gas reference obscures the physical meaning of the ELF.

Recently it has turned out that it is possible to define a localizability measure, called the electron localizability indicator (ELI), that reproduces the ELF formula in case of the HF wavefunction but without refering to the uniform electron gas [3]. This new definition possesses another appealing feature—it may be immediately extended to correlated wavefunctions.

The key idea in developing the ELI was to divide the whole space into a finite number of regions, each containing the same (fixed) small amount of σ-spin charge [3, 4, 5]. Subsequently, the integral of the same-spin electron pair density over such a region was determined by Taylor expansion of the pair density around the electron coalescence point. The integration yields the so-called q-restricted pair population from which the ELI is constructed without a reference to the uniform electron gas [3].

At the HF level the ELI, $\mathrm{ELF_{BE}}$, and $\mathrm{ELF_S}$ are apparently given by the same equation. Nevertheless, the $\mathrm{ELF_S}$ is a function of the electron density, whereas the $\mathrm{ELF_{BE}}$ and ELI are based on the electron pair density. Moreover, the $\mathrm{ELF_{BE}}$, an approximation to the ELI [3], is a function of the pair density (the curvature of the Fermi hole at the electron coalescence point), whereas the ELI is a functional of the pair density (a specific integral). For correlated wavefunctions the distinctions between the ELI and the ELF will be revealed.

With this new measure of electron localizability at hand, it is now feasible to investigate how the inclusion of the Coulomb correlation, that is absent in a HF wavefunction, influences the localizability of electrons in atoms and molecules. In the Theory part of this paper we present the extended formula for the ELI within the framework of configuration interaction (CI). In the application part we present the results for a few atoms and molecules obtained by means of the parallel-spin ELI applied to the correlated wavefunctions and compare them with the results obtained from Savin's formula via natural orbitals. Additionally, we have derived the ELI formula for a highly accurate Hylleraas-type

---

Correspondence to: M. Kohout
e-mail: kohout@cpfs.mpg.de

wavefunction to describe the shell structure of the helium atom in a triplet state.

2. Theory

Consider a wavefunction $\Psi(\mathbf{x}_1\mathbf{x}_2\cdots\mathbf{x}_N)$ describing a system composed of N electrons, where $\mathbf{x}_i=(\mathbf{r}_i,\sigma_i)$ comprises the spatial and spin coordinates $\mathbf{r}_i$ and σ_i, respectively, pertaining to the electron i. The wavefunction determines the spinless one- and two-electron reduced density matrices $\rho_1(\mathbf{r}_1'\mid\mathbf{r}_1)$ and $\rho_2(\mathbf{r}_1'\mathbf{r}_2'\mid\mathbf{r}_1\mathbf{r}_2)$, respectively [6,7,8]:

$$\begin{aligned}\rho_1(\mathbf{r}_1'\mid\mathbf{r}_1)&=N\int d\sigma_1\int d\mathbf{x}_2\cdots\\&\quad\times\int d\mathbf{x}_N\Psi^*(\mathbf{x}_1'\mathbf{x}_2\cdots\mathbf{x}_N)\Psi(\mathbf{x}_1\mathbf{x}_2\cdots\mathbf{x}_N)\\\rho_2(\mathbf{r}_1'\mathbf{r}_2'\mid\mathbf{r}_1\mathbf{r}_2)&=\binom{N}{2}\int d\sigma_1\int d\sigma_2\int d\mathbf{x}_3\cdots\\&\quad\times\int d\mathbf{x}_N\Psi^*(\mathbf{x}_1'\mathbf{x}_2'\cdots\mathbf{x}_N)\Psi(\mathbf{x}_1\mathbf{x}_2\cdots\mathbf{x}_N).\end{aligned}\tag{1}$$

The diagonal parts of those reduced density matrices are the electron density and the electron pair density:

$$\begin{aligned}\rho(\mathbf{r}_1)&=\rho_1(\mathbf{r}_1\mid\mathbf{r}_1)\\\rho_2(\mathbf{r}_1,\mathbf{r}_2)&=\rho_2(\mathbf{r}_1\mathbf{r}_2\mid\mathbf{r}_1\mathbf{r}_2).\end{aligned}\tag{2}$$

Note that the electron density is normalized to the number of electrons N, whereas the pair density normalizes to the number of electron pairs $N(N-1)/2$. Both densities may be decomposed into spin components [8] that are probability densities of finding one (in case of the electron density) or two (in case of the pair density) electrons with the respective spins in position space. The nonrelativistic total electron density can be decomposed into two spin components ρ_α (describing the density of electrons with spin up) and ρ_β (spin down)

$$\rho(\mathbf{r})=\rho_\alpha(\mathbf{r})+\rho_\beta(\mathbf{r}).\tag{3}$$

The pair density, on the other hand, can be decomposed into four spin components

$$\begin{aligned}&\rho_2(\mathbf{r}_1,\mathbf{r}_2)=\\&\quad\rho_2^{\alpha\alpha}(\mathbf{r}_1,\mathbf{r}_2)+\rho_2^{\beta\beta}(\mathbf{r}_1,\mathbf{r}_2)+\rho_2^{\alpha\beta}(\mathbf{r}_1,\mathbf{r}_2)+\rho_2^{\beta\alpha}(\mathbf{r}_1,\mathbf{r}_2).\end{aligned}\tag{4}$$

Let us consider a normalized CI wavefunction

$$\Psi(\mathbf{x}_1\cdots\mathbf{x}_N)=\sum_K C_K\Phi_K(\mathbf{x}_1\cdots\mathbf{x}_N),\tag{5}$$

where $K=k_1\cdots k_N$ represents an ordered string of N indices such that $k_1<\cdots<k_N$, and

$$\Phi_K(\mathbf{x}_1\cdots\mathbf{x}_N)=(N!)^{-1/2}|\phi_{k_1}(\mathbf{x}_1)\cdots\phi_{k_N}(\mathbf{x}_N)|\tag{6}$$

is a normalized Slater determinant constructed from the real-valued orthonormal spin orbitals ϕ_{k_i}. Although the sum in Eq. (5) runs through ordered (thus different) strings K, we assume for convenience that the coefficients C_K are antisymmetrical with respect to the permutation of any two indices in a string K as required by the antisymmetry of the wavefunction. Φ_K equals zero if two or more indices in K are the same. The normalization of Ψ requires that

$$\sum_K (C_K)^2=1.\tag{7}$$

The same-spin component $\rho_2^{\sigma\sigma}(\mathbf{r}_1,\mathbf{r}_2)$ of the electron pair density corresponding to the previous ansatz for the wavefunction reads (with $\sigma=\alpha,\beta$)

$$\begin{aligned}&\rho_2^{\sigma\sigma}(\mathbf{r}_1,\mathbf{r}_2)=\\&\quad\frac{1}{2}\sum_{i<j}^{\sigma}\sum_{k<l}^{\sigma}P_{ij,kl}|\phi_i(\mathbf{r}_1)\phi_j(\mathbf{r}_2)||\phi_k(\mathbf{r}_1)\phi_l(\mathbf{r}_2)|,\end{aligned}\tag{8}$$

where

$$P_{ij,kl}=\sum_{K'}C_{K'ij}C_{K'kl},\tag{9}$$

with $K'=k_1\cdots k_{N-2}$ (i.e., K' is the common substring of the coefficient indexes). Therefore the coefficients $P_{ij,kl}$ involve products C_KC_L of all coefficients differing at most by the indices i,j and k,l in the strings K and L.

Let us divide the space into compact mutually exclusive space-filling regions $\Omega_{\mathrm{q},a}$ (referenced by the point $\mathbf{r}_a$ inside the region), each containing the same small fixed σ-spin charge q_σ. To calculate the ELI, the q_σ-restricted pair population $\zeta^{\sigma}_{\mathrm{q,CI}}(\mathbf{r}_a)$, i.e., the same-spin pair population in $\Omega_{\mathrm{q},a}$ needs to be determined. The fixed charge condition ensures that, in the case of "uncorrelated" motion of the same-spin electrons, the q_σ-restricted pair population yields the same value $\zeta^{\sigma}_{\mathrm{q,CI}}(\mathbf{r}_a)=q_\sigma^2/2$ for all regions $\Omega_{\mathrm{q},a}$ [3].

Owing to the Pauli exclusion principle and the cusp condition [9,10], the Taylor expansion of the same-spin pair density at the electron coalescence point begins from the second-order term. Thus, utilizing the first non vanishing term of this Taylor expansion yields

$$\zeta^{\sigma}_{\mathrm{q,CI}}(\mathbf{r}_a)\approx\frac{1}{2}\iint_{\Omega_{\mathrm{q},a}}(\mathbf{s}\cdot\nabla_{\mathbf{r}_2})^2\rho_2^{\sigma\sigma}(\mathbf{r}_1,\mathbf{r}_2)\Big|_{\mathbf{r}_2\to\mathbf{r}_1}d\mathbf{r}_1d\mathbf{r}_2,\tag{10}$$

with

$$(\mathbf{s}\cdot\nabla_{\mathbf{r}_2})^2=\sum_{\mu,\nu}^{x,y,z}(\mu_2-\mu_1)(\nu_2-\nu_1)\frac{\partial^2}{\partial\mu_2\partial\nu_2},\tag{11}$$

where $\mathbf{s}=\mathbf{r}_2-\mathbf{r}_1$, $\mu_1=x_1,y_1,z_1$ and $\mu_2=x_2,y_2,z_2$ (and similarly for ν), respectively [3]. The nabla operator in the equations is acting on the coordinate $\mathbf{r}_2$ only. Inserting the pair density from Eq. (8) into Eq. (10), we obtain

$$\begin{aligned}\zeta^{\sigma}_{\mathrm{q,CI}}(\mathbf{r}_a)&\approx\frac{1}{4}\sum_{i<j}^{\sigma}\sum_{k<l}^{\sigma}P_{ij,kl}\sum_{\mu,\nu}^{x,y,z}\int_{\Omega_{\mathrm{q},a}}d\mathbf{r}_1D^{\mu,\nu}_{ij,kl}(\mathbf{r}_1)\\&\quad\times\int_{\Omega_{\mathrm{q},a}}(\mu_2-\mu_1)(\nu_2-\nu_1)d\mathbf{r}_2.\end{aligned}\tag{12}$$

The function $D^{\mu,\nu}_{ij,kl}(\mathbf{r}_1)$ is built from the i,j,k,l spin orbitals and the respective first μ and ν derivatives:

$$\begin{aligned}D^{\mu,\nu}_{ij,kl}(\mathbf{r}_1)&=[\phi_i(\mathbf{r}_1)\phi_j(\mathbf{r}_1)'^{\mu}-\phi_j(\mathbf{r}_1)\phi_i(\mathbf{r}_1)'^{\mu}]\\&\quad\times[\phi_k(\mathbf{r}_1)\phi_l(\mathbf{r}_1)'^{\nu}-\phi_l(\mathbf{r}_1)\phi_k(\mathbf{r}_1)'^{\nu}]\\&\quad+[\phi_i(\mathbf{r}_1)\phi_j(\mathbf{r}_1)'^{\nu}-\phi_j(\mathbf{r}_1)\phi_i(\mathbf{r}_1)'^{\nu}]\\&\quad\times[\phi_k(\mathbf{r}_1)\phi_l(\mathbf{r}_1)'^{\mu}-\phi_l(\mathbf{r}_1)\phi_k(\mathbf{r}_1)'^{\mu}]\end{aligned}\tag{13}$$

The second derivatives that result from the application of the operator $(\mathbf{s}\cdot\nabla_{\mathbf{r}_2})^2$ (Eq. 11) onto the same-spin pair density in Eq. (10), vanish for the CI ansatz after setting $\mathbf{r}_2$ to $\mathbf{r}_1$. This can easily be shown using the expansion of the same-spin pair density into products of determinants (Eq. 8). Let us denote the two determinants $|\phi_i(\mathbf{r}_1)\phi_j(\mathbf{r}_2)|$ and $|\phi_k(\mathbf{r}_1)\phi_l(\mathbf{r}_2)|$ by d_{ij} and d_{kl}, respectively. The second derivative with respect to μ_2 and v_2 of each product $d_{ij}d_{kl}$ is

$$\begin{aligned}\frac{\partial^2}{\partial\mu_2\partial v_2}(d_{ij}d_{kl}) = (d_{ij})'^{\mu_2}(d_{kl})'^{v_2} + (d_{ij})'^{v_2}(d_{kl})'^{\mu_2}\\ + d_{ij}(d_{kl})''^{\mu_2 v_2} + (d_{ij})''^{\mu_2 v_2}d_{kl}.\end{aligned} \tag{14}$$

In this expression the second $\mu_2 v_2$ derivative of a determinant is multiplied by the other determinant, for instance $(d_{ij})''^{\mu_2 v_2}d_{kl}$. These terms vanish after setting $\mathbf{r}_2$ to $\mathbf{r}_1$, because the determinants d_{kl} equal zero in this case.

The functions $D^{\mu,v}_{ij,kl}(\mathbf{r}_1)$ can be approximated by a Taylor expansion around the position $\mathbf{r}_a$ in the region $\Omega_{\mathrm{q},a}$. The zero-order terms of this expansion are the expressions $D^{\mu,v}_{ij,kl}(\mathbf{r}_a)$. Then, the q_σ-restricted pair population can be approximated by

$$\zeta^\sigma_{\mathrm{q,CI}}(\mathbf{r}_a) \approx \frac{1}{12}V(\Omega_{\mathrm{q},a})^{8/3}g(\mathbf{r}_a) + X(\Omega_{\mathrm{q},a}), \tag{15}$$

with

$$\begin{aligned}g(\mathbf{r}_a) = \sum_{i<j}^{\sigma}\sum_{k<l}^{\sigma}P_{ij,kl}\\ \times[\phi_i(\mathbf{r}_a)\nabla\phi_j(\mathbf{r}_a) - \phi_j(\mathbf{r}_a)\nabla\phi_i(\mathbf{r}_a)]\\ \cdot[\phi_k(\mathbf{r}_a)\nabla\phi_l(\mathbf{r}_a) - \phi_l(\mathbf{r}_a)\nabla\phi_k(\mathbf{r}_a)].\end{aligned} \tag{16}$$

The first term in Eq. (15) is proportional to the 8/3 power of the volume $V(\Omega_{\mathrm{q},a})$ of the region $\Omega_{\mathrm{q},a}$. It originates from the second-order term of the Taylor expansion of the same-spin pair density around the position $\mathbf{r}_1$, combined with the zero-order terms of the Taylor expansion of the functions $D^{\mu,v}_{ij,kl}(\mathbf{r}_1)$, i.e., the $\mathbf{r}_1$-independent expressions $D^{\mu,v}_{ij,kl}(\mathbf{r}_a)$, included in the integrals of Eq. 12 for which $\mu = v$. All the other integrals are collected in $X(\Omega_{\mathrm{q},a})$ which is proportional to the powers of $V(\Omega_{\mathrm{q},a})$ higher than 8/3.

The regions $\Omega_{\mathrm{q},a}$ are controled by the fixed charge condition, i.e., each of the (compact) regions $\Omega_{\mathrm{q},a}$ contain the same σ-spin charge q_σ [3]. For q_σ small enough the volumes of the regions are inversely proportional to the electron density, $V(\Omega_{\mathrm{q},a}) \approx q_\sigma/\rho_\sigma(\mathbf{r}_a)$. Thus, for a sufficiently small q_σ all integrals in $X(\Omega_{\mathrm{q},a})$ can be omitted. The q_σ-restricted pair population for a CI wavefunction reduces to

$$\zeta^\sigma_{\mathrm{q,CI}}(\mathbf{r}_a) \approx \frac{1}{12}q_\sigma^{8/3}\frac{1}{\rho_\sigma(\mathbf{r}_a)^{8/3}}g(\mathbf{r}_a). \tag{17}$$

In the HF approximation only one determinant is used and $P_{ij,kl} = \delta_{ik}\delta_{jl}$. The q_σ-restricted pair population for a HF wavefunction

$$\begin{aligned}\zeta^\sigma_{\mathrm{q,HF}}(\mathbf{r}_a) \approx \frac{1}{12}q_\sigma^{8/3}\frac{1}{\rho_\sigma(\mathbf{r}_a)^{8/3}}\\ \times\sum_{i<j}^{\sigma}[\phi_i(\mathbf{r}_a)\nabla\phi_j(\mathbf{r}_a) - \phi_j(\mathbf{r}_a)\nabla\phi_i(\mathbf{r}_a)]^2\end{aligned} \tag{18}$$

offers an appealing alternative to the usual formulation using $\tilde{t}_{\mathrm{P},\sigma}(\mathbf{r})$, i.e., the term resembling the Pauli kinetic energy density [3]. Notice that

$$\begin{aligned}\rho_\sigma\tilde{t}_{\mathrm{P},\sigma} &= \rho_\sigma\frac{1}{2}\sum_{k}^{\sigma}|\nabla\phi_i|^2 - \frac{1}{8}(\nabla\rho_\sigma)^2\\ &= \frac{1}{2}\sum_{i<j}^{\sigma}[\phi_i\nabla\phi_j - \phi_j\nabla\phi_i]^2.\end{aligned} \tag{19}$$

This opens the possibility to analyze the contributions of orbital pairs to the ELF or the ELI, respectively.

The q_σ-restricted pair population $\zeta^\sigma_{\mathrm{q,CI}}(\mathbf{r}_a)$ enters the ELI formula for a correlated wavefunction:

$$\Upsilon^\sigma(\mathbf{r}_a) = \frac{1}{1 + \left[c_\mathrm{q}\zeta^\sigma_{\mathrm{q,CI}}(\mathbf{r}_a)\right]^2}. \tag{20}$$

The factor c_q compensates the q_σ dependency of $\zeta^\sigma_{\mathrm{q,CI}}(\mathbf{r}_a)$ and makes the ELI and ELF values identical at the HF level of calculation [3]:

$$c_\mathrm{q} = \frac{6}{(3/5)(6\pi^2)^{2/3}q_\sigma^{8/3}}. \tag{21}$$

The same-spin pair density can be written in the following form:

$$\begin{aligned}\rho_2^{\sigma\sigma}(\mathbf{r}_1,\mathbf{r}_2) = \frac{1}{2}\left[\rho_\sigma(\mathbf{r}_1)\rho_\sigma(\mathbf{r}_2) - \left|\rho_1^\sigma(\mathbf{r}_1|\mathbf{r}_2)\right|^2\right]\\ + \chi_{\sigma\sigma}(\mathbf{r}_1,\mathbf{r}_2),\end{aligned} \tag{22}$$

where the term in the square brackets is the σ-component of the generalized HF matrix ρ_2^{GHF}, whereas $\chi_{\sigma\sigma}(\mathbf{r}_1,\mathbf{r}_2)$ is the diagonal part of the same-spin component of the cumulant density matrix [11,12,13]. The generalized HF matrix may be easily expressed in terms of the natural orbitals $\varphi_i(\mathbf{r})$ (assumed to be real-valued) and natural occupation numbers n_i that are, respectively, eigenvectors and eigenvalues of the one-electron reduced density matrix (Eq. 1):

$$\begin{aligned}\rho_2^{GHF}(\mathbf{r}_1,\mathbf{r}_2) =\\ \frac{1}{2}\sum_{i<j}^{\sigma}n_i n_j[\varphi_i(\mathbf{r}_1)\varphi_j(\mathbf{r}_2) - \varphi_j(\mathbf{r}_1)\varphi_i(\mathbf{r}_2)]^2.\end{aligned} \tag{23}$$

Using the pair density from Eq. (22) in the derivation of the q_σ-restricted pair population $\zeta^\sigma_{\mathrm{q,CI}}$ (Eqs. 17, 18) yields

$$\begin{aligned}\zeta^\sigma_{\mathrm{q,CI}}(\mathbf{r}_a) \approx \frac{1}{12}q_\sigma^{8/3}\frac{1}{\rho_\sigma(\mathbf{r}_a)^{8/3}}\\ \times\left[\sum_{i<j}^{\sigma}n_i n_j[\varphi_i(\mathbf{r}_a)\nabla\varphi_j(\mathbf{r}_a) - \varphi_j(\mathbf{r}_a)\nabla\varphi_i(\mathbf{r}_a)]^2\right.\\ \left.+ \nabla^2_{\mathbf{r}_2}\chi_{\sigma\sigma}(\mathbf{r}_a,\mathbf{r}_2)\Big|_{\mathbf{r}_2\to\mathbf{r}_a}\right].\end{aligned} \tag{24}$$

The sum in the square brackets in Eq. (24) is actually twice $\rho_\sigma\tilde{t}_{\mathrm{P},\sigma}$ computed from the natural orbitals (Eq. 19).

The $\mathrm{ELF_S}$ in the formulation of Savin et al. [2] is based on the Pauli kinetic energy density of noninteracting electrons using Kohn–Sham orbitals. In analogy to the $\mathrm{ELF_S}$ the natural orbitals can be used to compute the Pauli kinetic energy density (now for interacting electrons). Leaving the $\rho_\sigma^{5/3}$ reference (from the ELF$_S$) unchanged yields the formula ELF$_{SI}$ (i.e., the ELF$_S$ for interacting electrons). The ELF$_{SI}$ equals the ELI after neglecting the Laplacian of the cumulant matrix in Eq. (24).

3. Results

Our aim is to elucidate the principles of the proposed approach to describe the localizability for correlated functions. A few examples were chosen to manifest the differences between the ELI and the ELF, respectively, without the objective to present the results for the best optimized wavefunctions. The quantum chemical calculations were performed with the Gaussian 98 package [14] using the aug-cc-pVTZ basis set. The ELF and the ELI were computed from the Gaussian results with the program DGrid [15], which was extended to evaluate the CI vectors and configuration lists according to Eqs. (17) and (20). The localizability basins were determined with the program Basin [16].

3.1 H_2 molecule

The wavefunction for the ground state $^1\Sigma_g^+$ of the H_2 molecule is occupied by two electrons with opposite spins. The absence of the same-spin electron pair consequently implies zero q_σ-restricted pair population, yielding ELI values equal to 1 everywhere in space for both, the HF and the CI ansatz. The same result is given for the ELF computed from the HF wavefunction.

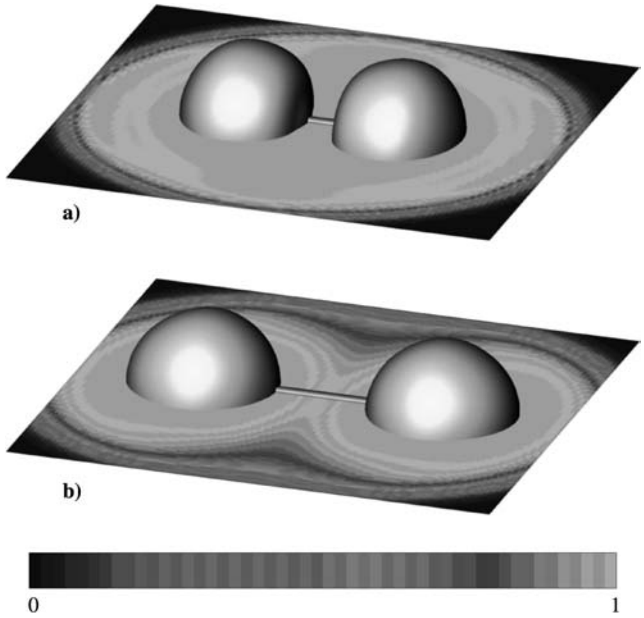

Fig. 1 Electron localization function for interacting electrons (ELF$_{SI}$) for the H_2 molecule (0.999-localization domains) using the CASSCF(2,6) wavefunction of the ground state $^1\Sigma_g^+$. The colormap applies to the slices in all diagrams. **a** Bond distance of 75 pm. **b** Bond distance of 150 pm. *Red line* H–H bond axis

However, a very distinctive ELF$_{SI}$ distribution is obtained for the CI wavefunction. Because of the fractional occupation numbers of the natural orbitals, more than one orbital is involved in the term $\sum_{i<j}^{\sigma} n_i n_j [\phi_i \nabla \phi_j - \phi_j \nabla \phi_i]^2$, cf. Eq. (24), yielding a nonzero sum value. A complete-active-space self-consistent-field (CASSCF) calculation of H_2 using six orbitals (namely $1\sigma_g$, $2\sigma_g$, $1\sigma_u$, $2\sigma_u$, $1\pi_{ux}$, and $1\pi_{uy}$), i.e., CASSCF(2,6) in Gaussian notation, involves 36 Slater determinants. The calculation yields six natural orbitals, whereby the lowest two orbitals are occupied by 1.968 and 0.023 electrons (both spins) at the bond distance of 75 pm, and by 1.817 and 0.176 electrons at 150 pm, respectively. Figure 1 shows the 0.999-localization domains (i.e., space regions bounded by ELF$_{SI}$ isosurfaces with $\eta = 0.999$) for the two bond distances. The ELF$_{SI}$ distribution is no longer uniform. Instead, the localization domains visualize two hydrogen atoms without an attractor between the protons. Loosely speaking, in this case the ELF$_{SI}$ computed from natural orbitals seems to describe "pairs" formed between fractional (physically nonexistent) parts of electrons. Thus, the ELF$_{SI}$ represents some electron density property, different from the correlation of motion of the same-spin electrons.

3.2 N_2 molecule

The active space for the CASSCF(10,8) calculation of the ground state, $^1\Sigma_g^+$, of the N_2 molecule consisted of the orbitals $2\sigma_g$, $3\sigma_g$, $2\sigma_u$, $3\sigma_u$, $1\pi_{ux}$, $1\pi_{uy}$, $1\pi_{gx}$, and $1\pi_{gy}$ (bond distance of 111 pm) [17]. The calculation involved 3136 Slater determinants.

The ELF$_{SI}$ computed from the resulting ten natural orbitals (the virtual orbitals are occupied by 0.067 and 0.020 electrons, respectively) exhibits high values in the regions of the atomic cores as well as in the bonding region between the cores and in the region that can be attributed to the lone electron pairs (Fig. 2a). Apart from the bond distance (107 pm [17]) it resembles the HF results [18]. Even the electron count of 3.44 electrons for the basin in the bond region remains almost unchanged with respect to the HF calculation (3.47 electrons [19]).

The overall picture remains the same using the ELI for this small active space calculation. The ELI values in the bond and lone pair regions are only slightly higher than the corresponding ELF values. Consequently, as shown in Fig. 2b, the 0.80-localization domains are only marginally larger than the corresponding ELF domains. The electron count for the ELI bond basin is the same as the one for the ELF bond basin. To get an electron count of six electrons ("expected" for the triple bond) a considerable shift in the zero-flux surface separating the bond from the "lone" pair would be needed. Disregarding the argument that there is no theoretical background for this "bond order–electron count" correspondence, it remains an open question whether a large-scale multireference CI could yield this shift. This will be the subject of further investigation.

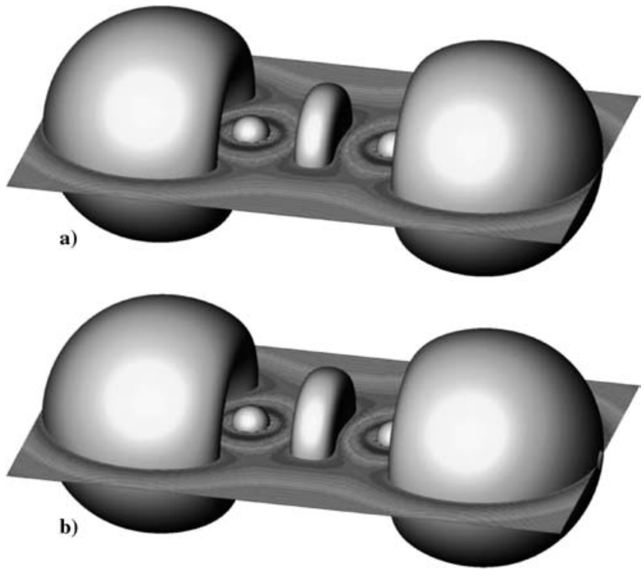

Fig. 2 0.80-localization domains for the ground state ${}^1\Sigma_g^+$ of the N_2 molecule. **a** ELF_{SI}. **b** Electron localizability indicator (ELI)

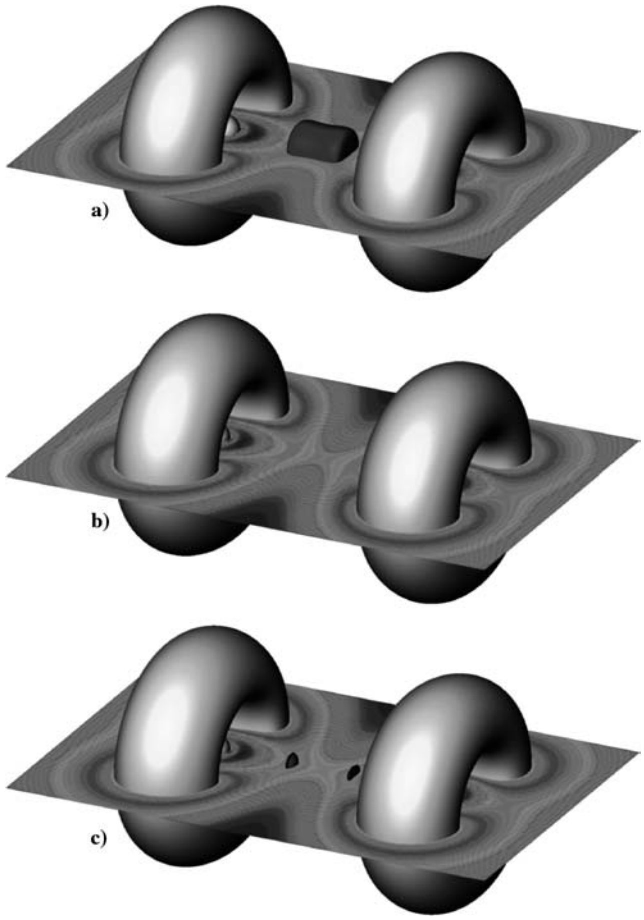

Fig. 3 The ground state ${}^1\Sigma_g^+$ of the F_2 molecule. The *gold* isosurfaces are the 0.85-localization domains. **a** ELF from the Hartree-Fock calculation. The *red* 0.65-localization domain encloses the bond attractor. **b** ELF_{SI} from the natural orbitals. **c** ELI. The *red* 0.6136-localization domains enclose one "bifurcated" bond attractor

The electron counts are affected by the change of the geometric shape of the particular basins, i.e., by the position of the zero-flux surfaces, which in turn are determined by the values of the localizability indicator. However, the value of the localizability indicator, Eq. (20), does not scale linearly with the q_σ independent functional $c_q \zeta^\sigma_{q,CI}(\mathbf{r}_a)$, in the following denoted by χ. We emphasize this for the reason that small changes of χ, due to the inclusion of the electron correlation, are preferably perceivable at high (i.e., close to 1) ELI values only. In this case, small changes of the ELI are caused by changes of χ^2 of approximately the same magnitude. In contrast, for low ELI values (i.e., close to 0) small changes of the ELI are due to relatively large changes of χ^2. For convenience, let us look at two examples considering the difference of 0.01 with respect to the ELI values 0.98 and 0.01, respectively. The increase of the ELI value from 0.98 to 0.99 is due to the tiny decrease of χ^2 from 0.02 to 0.01, whereas the increase of the ELI value from 0.01 to 0.02 is connected with the large decrease of χ^2 from 99 to 49. Thus, the inclusion of the electron correlation can modify the topology of the ELI distribution at high values, but it probably will have only a minor effect on the surfaces of zero flux in the ELI gradient (ELI basins) controlled by regions of low ELI.

3.3 F_2 molecule

For the ground state ${}^1\Sigma_g^+$ of the F_2 molecule the same active space as for N_2 was used. Thus, 64 Slater determinants were involved in the CASSCF(14,8) calculation (bond distance 146 pm [17]).

Figure 3a shows the ELF for the HF calculation (bond distance of 133 pm [17]). Besides the core and lone pair regions, visualized by the 0.85-localization domains, a separate bond region depicted by the 0.65-localization domain (red) around the ELF maximum at the bond midpoint is well discernible. The integration of the electron density in the bond basin yields an electron count of merely 0.9 electrons. The topology around the attractor is flat: the ELF curvature in the bond direction is small in magnitude, which already indicates potential instability of the attractor towards bifurcation catastrophe (i.e., splitting of the bond attractor, see the later discussion of the ELI).

In Fig. 3b, showing ELF_{SI} computed from the natural orbitals (CASSCF calculation), the core and lone pair regions are still clearly recognizable. But one important feature is missing: an ELF_{SI} attractor representing the F–F bond. Instead, there is an ELF_{SI} saddle point at the midpoint between the cores. This can be rationalized bearing in mind that the active space of the occupied HF orbitals was extended by the virtual antibonding orbital $3\sigma_u$.

Figure 3c displays the ELI for the CASSCF calculation. Apparently, besides the cores and lone pairs, two ELI attractors are present along the bond axis between the cores, facing each other. This new feature is visualized by the red 0.6136-localization domains enclosing the "bifurcated" bond attractor.

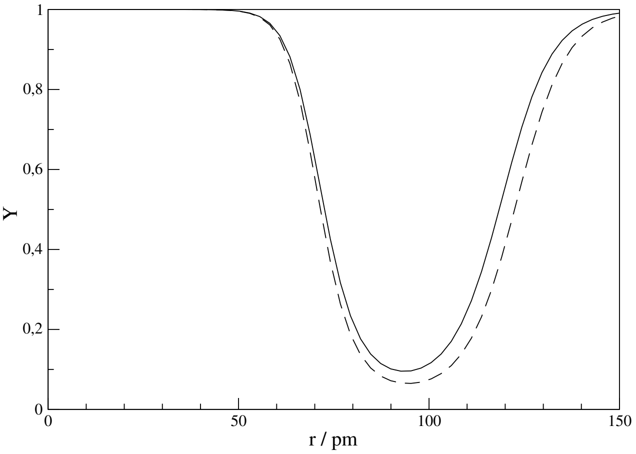

Fig. 4. Atomic shell structure as shown by the ELI for the 2^3S state of helium using Hylleraas functions. *Dashed line* six-parameter function; *solid line* 32-parameter function

Using a shorter bond distance in the CASSCF calculation (for instance the one for the HF results) also yields the bifurcated bond attractor in the $\mathrm{ELF}_{\mathrm{SI}}$ distribution. But the volume of the largest irreducible localization domains assigned to the bifurcated bond attractor (i.e., just before the localization domains for the bifurcated bond attractor join the lone pair domain) is always higher for the ELI. The same applies for the extension of the active space of CASSCF by additional virtual orbitals.

3.4 He atom

The q_σ-restricted pair population $\zeta^{\sigma}_{\mathrm{q,CI}}(\mathbf{r}_a)$–the basic ingredience of the ELI—is given as the volume integral of the electron pair density. Thus, the ELI is independent of the actual representation of the pair density. To demonstrate this we present here the ELI for the $2^3\mathrm{S}$ state of the He atom described by Hylleraas functions. In this case the wavefunction (two same-spin electrons) is not decomposed into orbitals. Instead, the Hylleraas function $\Psi(r_1, r_2, r_{12})$ explicitly includes the distance r_{12} between the electrons [20]. Because of the spherical symmetry, only two additional variables are needed, namely the distances r_1 and r_2 of each electron to the nucleus.

As already described in the Theory section, the second-order term of the Taylor expansion of the same-spin pair density ρ_2 around the coalescense point is needed to approximate the q_σ-restricted pair population. Because of the spherical symmetry the Laplacian can be written as $\partial^2/\partial r^2 + 2/r(\partial/\partial r)$. Bearing in mind that at the coalescence ($r_{12} = 0$) the gradient of the Fermi hole is zero, the Laplacian of the same-spin pair density (ρ_2 is given as the squared Hylleraas function) will reduce to

$$\nabla^2_{\mathbf{r}_2}\rho_2\big|_{r_{12}\to 0} = \partial^2/\partial r_2^2\rho_2\big|_{r_{12}\to 0}. \qquad (25)$$

Besides the pair density Laplacian the electron density $\rho(r_1)$ must be known to compute the approximate value of $\zeta^{\sigma}_{\mathrm{q,CI}}(\mathbf{r}_a)$. For the ansatz of Hylleraas the electron density is given by the integral (omitting occasional constants that are sometimes included in Hylleraas functions)

$$\rho(r_1) = \frac{1}{r_1}\int_0^\infty dr_2 \int_{|r_1-r_2|}^{r_1+r_2} r_2 r_{12}\Psi^2(r_1, r_2, r_{12})dr_{12}. \qquad (26)$$

We have used two different Hylleraas functions: the six-parameter function of Traub and Foley [21] and the 32-parameter function of Ermolaev and Sochilin [22], respectively. The latter ansatz includes logarithmic functions. As shown in Fig. 4, the ELI exhibits in both cases the atomic shell structure [23]. The ELI minimum for the 32-parameter function, at 93.6 pm, is somewhat closer to the nucleus than the one for the six-parameter function (at 94.5 pm). The integration of the electron density in the first atomic shell, i.e., from the nucleus to the ELI minimum, yields 1.0061 electrons for the 32-parameter function. This is marginaly closer to the "ideal" electron count of one electron than the 1.0075 electrons for the six-parameter function.

4. Conclusions

The ELI is a functional of the same-spin electron pair density describing the local correlation of motion of same-spin electrons. The ELI is uniquely defined for any approach that yields the electron pair density. The ELI formula was derived in the framework of the configuration interaction ansatz. It differs (by the Laplacian of the cumulant matrix) from the $\mathrm{ELF}_{\mathrm{SI}}$ based on the Pauli kinetic energy density of interacting electrons. Similarity and difference between the ELI and the $\mathrm{ELF}_{\mathrm{SI}}$ were principally shown for examples of H_2, N_2, and F_2 molecules. The ELI based on Hylleraas functions was analyzed for the triplet state of the He atom, revealing quantitatively the atomic shell structure.

Acknowledgements. This study was supported by Deutsche Forschungsgemeinschaft. K.P. acknowledges the Young Scientist Fellowship from the Foundation for Polish Science and extends her thanks to the Max Planck Society for research fellowship.

References

1. Becke AD, Edgecombe KE (1990) J Chem Phys 92:5397
2. Savin A, Jepsen O, Flad J, Andersen OK, Preuss H, von Schnering HG (1992) Angew Chem 104:186
3. Kohout M (2004) Int J Quantum Chem 97:651
4. Dobson JF (1991) J Chem Phys 94:4328
5. Savin A, Nesper R, Wengert S, Fässler TF (1997) Angew Chem Int Ed Engl 36:1808
6. Löwdin, P.-O. Phys Rev (1955), 97, 1474.
7. Parr RG, Yang W (1989) Density-functional theory of atoms and molecules. Oxford University Press, Oxford
8. McWeeny R, Mizuno Y (1961) Proc R Soc Lond Ser A 259:554
9. Kimball JC (1973) Phys Rev A 7:1648
10. Rajagopal AK, Kimball JC, Banerjee M (1978) Phys Rev B 18:2339
11. Fulde P (1991) Electron correlation in molecules and solids. Springer, Berlin Heidelberg New York
12. Kutzelnigg W, Mukherjee D (1999) J Chem Phys 110:2800

13. Ziesche P (2000) In: Cioslowski J (ed) Many-electron densities and reduced density matrices. Kluver/Plenum, NewYork, and references therein
14. Frisch MJ, Trucks GW, Schlegel HB, Scuseria GE, Robb MA, Cheeseman JR, Zakrzewski VG, Montgomery JA Jr, Stratmann RE, Burant JC, Dapprich S, Millam JM, Daniels AD, Kudin KN, Strain MC, Farkas O, Tomasi J, Barone V, Cossi M, Cammi R, Mennucci B, Pomelli C, Adamo C, Clifford S, Ochterski J, Petersson GA, Ayala PY, Cui Q, Morokuma K, Malick DK, Rabuck AD, Raghavachari K, Foresman JB, Cioslowski J, Ortiz JV, Baboul AG, Stefanov BB, Liu G, Liashenko A, Piskorz P, Komaromi I, Gomperts R, Martin RL, Fox DJ, Keith T, Al-Laham MA, Peng CY, Nanayakkara A, Gonzalez C, Challacombe M, Gill PMW, Johnson B, Chen W, Wong MW, Andres JL, Gonzalez C, Head-Gordon M, Replogle ES, Pople JA (1998) Gaussian 98, revision A.7. Gaussian, Pittsburgh, PA
15. Kohout M (2003) Program DGrid, version 2.4. Max-Planck-Institut für Chemische Physik fester Stoffe, Dresden
16. Kohout M (2003) Program Basin, version 2.4. Max-Planck-Institut für Chemische Physik fester Stoffe, Dresden
17. Peterson KA, Kendall RA, Dunning TH Jr (1993) J Chem Phys 99:9790
18. Savin A, Becke AD, Flad J, Nesper R, Preuss H, von Schnering HG (1991) Angew Chem 103:421
19. Chesnut DB (2001) Chem Phys 271:9
20. Hylleraas EA (1929) Z Phys 54:347
21. Traub J, Foley HM (1958) Phys Rev 111:1098
22. Ermolaev AM, Sochilin GB (1968) Int J Quantum Chem 2:333
23. Kohout M, Savin A (1996) Int J Quantum Chem 60:875